

Cross Sections for Dielectronic Recombination of B^{2+} and C^{3+} via $2s \rightarrow 2p$ Excitation

P. F. Dittner, S. Datz, P. D. Miller, C. D. Moak, P. H. Stelson,
C. Bottcher, W. B. Dress, G. D. Alton, and N. Nešković^(a)

Physics Division, Oak Ridge National Laboratory, Oak Ridge, Tennessee 37830

and

C. M. Fou

Department of Physics, University of Delaware, Newark, Delaware 19711

(Received 21 March 1983)

Dielectronic recombination cross sections for the Li-like ions B^{2+} and C^{3+} via $1s^2 2s \rightarrow 1s^2 2p$ excitation are reported. The amount of electron capture attending the passage of megaelectronvolt/(atomic mass unit) ion beams through a collinear, magnetically confined, space-charge-limited electron beam is observed as a function of relative energy. The results agree well with distorted-wave calculations.

PACS numbers: 34.80.Dp, 34.90.+q

Dielectronic recombination (DR) is the process by which a continuum electron excites a bound electron in an ion A^{q+} and is simultaneously captured into a doubly excited state of the resulting ion $A^{(q-1)+}$. Recombination occurs when the doubly excited state is stabilized via the emission of a photon. Thus for Li-like ions undergoing $2s \rightarrow 2p$ excitation, the process can be written

$$A^{q+}(1s^2 2s) + e^- \\ = A^{(q-1)+}(1s^2 2pnl) + A^{(q-1)+}(1s^2 2snl) + h\nu.$$

The DR cross sections must be known in order to model correctly high-temperature plasmas such as those found in stellar coronas and controlled fusion devices. DR cross sections and rates based on the distorted-wave (DW) method^{1,2} have been calculated for only a small number of ions; most plasma modeling still uses the formula of Burgess and Merts (BM).³⁻⁵ Until now, however, there have been no direct cross-section measurements of DR involving multiply charged ions. Only recently the first measurements of DR in singly charged ions of carbon⁶ and magnesium⁷ have been reported.

The merged-beam apparatus is outlined in Fig. 1. A beam of ions from the Oak Ridge National Laboratory EN-tandem accelerator enters (through a 0.635-mm-diam hole in the cathode of the electron gun) a region, 84 cm long, in which the electron beam is magnetically confined. Thereafter, the electrons expand as a result of space-charge repulsion and strike the chamber walls while the ion beam is subjected to a charge analysis through magnetic deflection. The A^{q+} ions enter a Faraday cup and the $A^{(q-1)+}$

ions can be counted in a position-sensitive solid-state surface-barrier detector (PSD) with an efficiency of 100%. The overall length of the beam line is ~ 7 m and it is maintained at a pressure of $\sim 1 \times 10^{-9}$ Torr.

The doubly gridded Pierce-type high-intensity electron gun⁸ is designed to produce a convergent, laminar electron beam. The gun was operated in the space-charge-limited mode where the space-charge-limited current, I_c , is given in terms of the cathode to anode voltage, V_c , by $I_c = PV_c^{3/2}$. The constant P (the "perveance") is determined by the electrode geometry and here equals 10^{-6} . The electron gun is magnetically shielded from the solenoidal field of the interaction region. The emerging electron beam comes to a focus ~ 7 mm from the anode where it has a diameter (containing 95% of the beam) of 3.15 mm. It enters a coaxial solenoidal magnetic field which is adjusted to establish Brillouin flow⁹ (e.g. ~ 180 G for 1-keV electrons) in which the beam radius stays constant and the beam rotates as a solid of revolution about its axis with the Larmor frequency, ω_L . Under Brillouin flow, the longitudinal velocity of the electrons is independent of radius, the radial velocity is zero, and the azimuthal velocity is

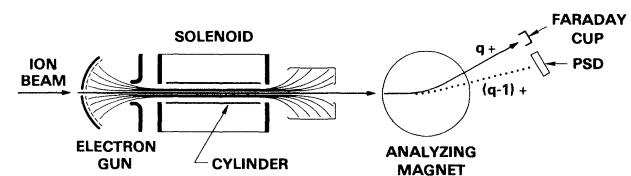


FIG. 1. Schematic diagram of the merged-beam apparatus.

equal to ω_L times the radius. Surrounding the electron beam is a coaxial cylinder 84 cm long having an inside diameter of 7.9 mm. Following the interaction region, the ions that have picked up an electron $A^{(q-1)+}$ are separated from the A^{q+} beam and counted in the PSD. The A^{q+} beam current to the Faraday cup is fed into a current integrator and the output pulses are counted. The $A^{(q-1)+}$ ions arise from electron pickup due to charge transfer from the residual gas molecules, slit-edge scattering, and DR.

The experimental procedure consisted of optimizing the electron beam, at a particular V_c , and counting the $A^{(q-1)+}$ and A^{q+} beams while stepping through the relative energies of interest by changing the energy of the ion beam. This optimization was carried out by adjusting the orientation of the solenoid, and making small adjustments to the solenoidal field such that the current to the cylinder was a minimum ($<0.1I_c$). It was then verified that the electrostatic field, due to the electron space charge, produced no steering of the ion beam. The deviation of the ratio, R , of $(q-1)+$ ions to $q+$ ions from a monotonic trend with ion beam energy gives a measure of the DR cross section. In Fig. 2 we plot this ratio for a C^{3+} beam (17.5–23 MeV) merged with an electron beam at $V_c = 1079$ V. (The error bar represents \sqrt{N} counting statistics.) The background ratio, R_B , can be fitted by a monotonic trend line (see, e.g., Fig. 2). Subtracting R_B from R yields the signal ratio R_s . R_s is re-

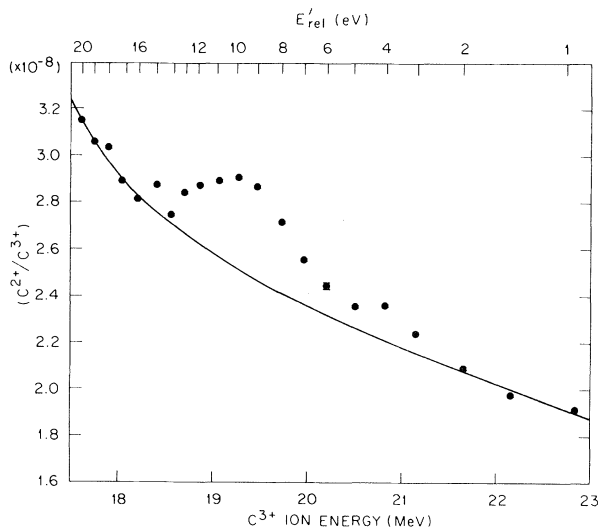


FIG. 2. Ratio C^{2+}/C^{3+} as a function of C^{3+} ion energy. See text for the definition of E'_{rel} .

lated to the DR cross section σ by

$$R_s = \iint \sigma(v_r) \rho_e \rho_i f(v_r) dv_r d\mathcal{V} / \int \rho_i v_i dA,$$

where ρ_e is the electron density, ρ_i is the ion density, v_r is the relative velocity, v_i is the velocity of the ions, and \mathcal{V} and A are the volume and cross-sectional area of the interaction region, a cylinder whose radius is that of the ion beam r_i , and having the length of the electron beam, L ; v_i is constant and the ion current I_i is given to a good approximation by $I_i = \pi r_i^2 \rho_i v_i$. Approximating ρ_e by an average electron density $\bar{\rho}_e$ times a distribution in relative velocities $f(v_r)$, both being independent of position within \mathcal{V} , we can write that $R_s = (\bar{\rho}_e L / v_i) \langle v_r \sigma \rangle$, and if we define an effective DR cross section, $\sigma_{eff} = \langle v_r \sigma \rangle / \langle v_r \rangle$, then we have $\sigma_{eff} = R_s v_i / (\bar{\rho}_e L \langle v_r \rangle)$, where the angular brackets denote the average over $f(v_r)$.

To compare the derived experimental σ_{eff} with theoretical calculations of the DR cross sections one must consider some details of both the experiment and the theory. DR in both B^{2+} and C^{3+} leaves the resulting B^{1+} and C^{2+} in excited states dominated by high- n states. The higher- n states were field ionized by the motional field caused by the magnetic field, B , used to separate the two charge states. To estimate the quantum number, n_{max} , above which field ionization occurs, we use the relation¹⁰ $n_{max} = (6.31 \times 10^{10} q^3 / v_i B)^{1/4}$ (mks units). The n_{max} values for our experimental conditions are listed in Table I.

If we neglect the potential difference due to space charge, the approximate relative collision energy, E_{rel}' , is given by $E_{rel}' = \frac{1}{2} m_e (v_c - v_i)^2$, where v_c is the electron velocity calculated from the applied cathode voltage, V_c . This energy is plotted along the top of Fig. 2. It can be seen that on this scale the peak of the resonance lies at ~ 10 eV, or ~ 3 eV above the expected peak energy of 7.1 eV. This occurs because the actual axial electron velocity, v_e , is determined not only by the potential applied to the cathode, V_c ,

TABLE I. Theoretical and experimental DR effective peak cross-section values for B^{2+} and C^{3+} ($\Delta E_{rel}' = 3$ eV).

Ion	n_{max}	σ_{eff} (10^{-19} cm ²)		
		BM	DW	Expt.
B^{2+}	22	2.6	1.1	1.0 ± 0.3
C^{3+}	26	4.0	1.6	2.1 ± 0.7

but also by the potential drop from the axis to the surrounding grounded cylinder, V_d : Thus $v_e = [2e(V_c - V_d)/m]^{1/2}$, where e and m are the charge and mass of the electron, respectively. This voltage drop, V_d , can be calculated if the net charge density, ρ , and radius, a , of the electron beam, and the inside radius, b , of the cylinder are known. Since some positive ions which are created by electron beam bombardment of background gas may be trapped in the space-charge trough, $|\rho|$ is equal to the electron density $|\rho_e|$ minus the trapped ion charge density $|\rho_t|$. The voltage drop V_d can be estimated from the shift in the resonance peak from its theoretical value. For $n < n_{\max}$ we have convoluted Gaussian distributions in relative energy $P(E_{\text{rel}})$ into the energy dependence of the cross sections predicted by DW theories and determined the predicted peak position. Note that this peak always lies very close to the $2s \rightarrow 2p$ excitation energy and is insensitive to $P(E_{\text{rel}})$ for a full width at half maximum, $\Delta E_{\text{rel}} > 1$ eV. We now force the experimental peak to this position and calculate the requisite voltage drop across the electron beam. For example, if we assume $\rho_t = 0$ we calculate a voltage drop $V_d = 47$ V at, e.g., $V_c = 1079$ V. If $\rho_t = \rho_e$, then the voltage drop is zero and the electron energy is just eV_c . From the shifts in the resonance peaks in two of our experiments using an identical electron beam at $V_c = 1079$ V, we obtain voltage drops of 31 and 29 V with B^{2+} and C^{3+} , respectively, thus indicating that we had some, but not complete, space-charge neu-

tralization. From the corrected value of v_e we recalculated the relative energy scales as shown in Figs. 3 and 4. The values of ΔE_{rel} which best fit the data were obtained and this permits direct comparison of the experimental σ_{eff} at the maximum with the theoretical predictions using the same ΔE_{rel} . A value of $\Delta E_{\text{rel}} = 3$ eV was found to give the best fit for all cases (five runs). For the B^{2+} case we plot in Fig. 3 the DW theoretical curve¹¹ normalized at the peak. For the C^{3+} case Ref. 2 predicts a large contribution to the cross section near threshold from the $2p4d$ and $2p4f$ configurations. This should cause a second rise in the signal at $E_{\text{rel}} \cong 1.5$ eV which we do not observe (note that the corrected value for $E_{\text{rel}} = 0$ lies at 22.5 MeV in Fig. 2). However, the configurations in question are known to have complicated multiplet structures most of whose levels lie below the autoionization limit¹² where they cannot contribute to the DR cross section. The BM theory predicts only a small cross section in this region. Because of these uncertainties we omit a theoretical plot in this region in Fig. 4. If there is indeed a contribution to the rate in this region we should correct the background in Fig. 2 downward in this energy range. This would increase the peak value in Fig. 4 only slightly. Table I summarizes and compares the peak values of σ_{eff} obtained in this experiment with the DW and BM theories.

We estimated the uncertainty in our determina-

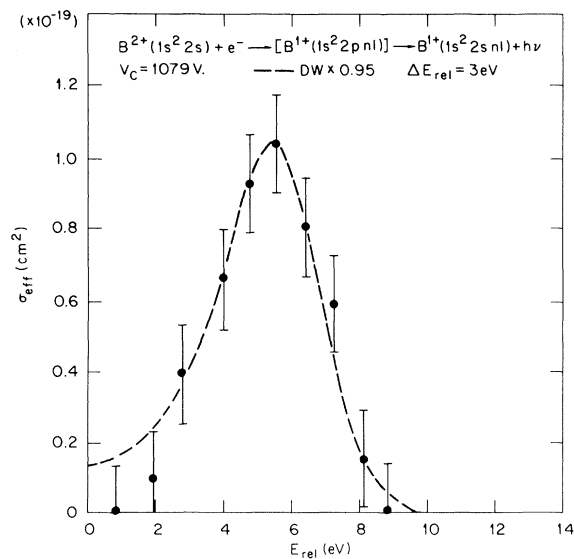


FIG. 3. σ_{eff} for DR in B^{2+} vs relative energy.

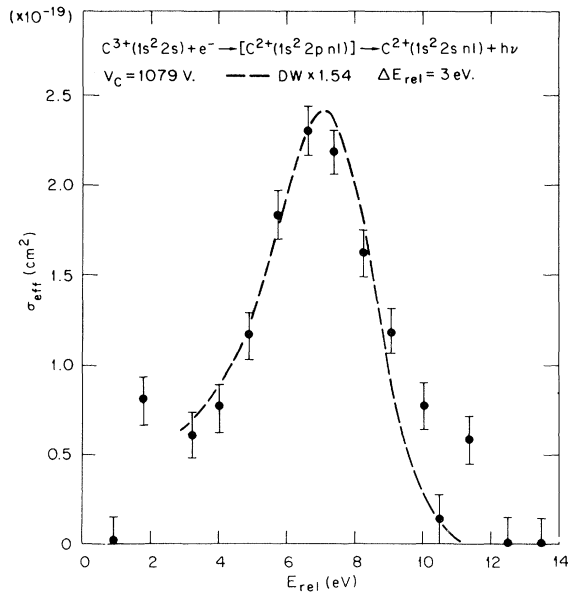


FIG. 4. σ_{eff} for DR in C^{3+} vs relative energy.

tion of σ_{eff} as follows: v_i is uncertain by <1% and v_r and L by 5%; the uncertainty due to statistics is 12% and 5% for B^{2+} and C^{3+} , respectively. The ρ_e was derived from measurements of the electron beam profile supplied by the manufacturer of the electron gun and from our own measurements using two rotatable Faraday cups placed along the length of the beam. Both cups indicated the same profile and were in reasonable agreement with the manufacturer's measurements. From these measurements we assign an uncertainty of 30% to ρ_e . Adding the errors in quadrature gave an uncertainty in σ_{eff} of 33% for B^{2+} and 31% for C^{3+} . Notwithstanding the uncertainties in the absolute value of the individual cross sections, the ratio $\sigma_{\text{eff}}(\text{C}^{3+})/\sigma_{\text{eff}}(\text{B}^{2+})$ is uncertain by only 13% since both experiments were carried out with the same electron beam conditions.

The quantitative agreement of our measurements with calculations is quite good. From the comparison of the cross-section ratios it can be seen that both calculations predict $\sigma_{\text{eff}}(\text{C}^{3+})/\sigma_{\text{eff}}(\text{B}^{2+}) = 1.5$ which is in slight disagreement with our value of 2.1 ± 0.3 .

The experimental approach used in this work (i.e., merging high-energy multiply charged ion beams with space-charge-limited electron beams) was undertaken because (1) multiply charged ions are easily obtained at megaelectronvolt/(atomic mass unit) energies, (2) charge transfer cross sections and hence backgrounds due to residual gas are greatly reduced at high ion velocities, (3) increased signals can be obtained with high-density electron beams, and (4) the space-charge-limited electron density increases as v_e^2 . Although some energy resolution was sacrificed because of the voltage drop over the radial region of electron-ion-beam overlap, this is not

a serious limitation in studying multicharged ions where peak widths become quite broad. We believe that the present results justify the approach taken and bode well for measurements on more highly charged species.

This research was sponsored by the U. S. Department of Energy, Division of Basic Energy Sciences under Contract No. W-7405-eng-26 with Union Carbide Corporation.

^(a)On leave from Boris Kidrič Institute, Belgrade, Yugoslavia.

¹K. LaGattuta and Y. Hahn, Phys. Rev. A 26, 1125 (1982).

²D. McLaughlin and Y. Hahn, Phys. Rev. A 27, 1389 (1983).

³A. Burgess, Astrophys. J. 139, 776 (1964).

⁴R. D. Cowan, *The Theory of Atomic Structure and Spectra* (Univ. of California Press, Berkeley, 1981); A. L. Merts, R. D. Cowan, N. H. Magee, Jr., Los Alamos Scientific Laboratory Report No. LA 6220-MS (unpublished).

⁵L. J. Roszman, in *Physics of Electronic and Atomic Collisions*, edited by S. Datz (North-Holland, Amsterdam, 1982), p. 641.

⁶J. B. A. Mitchell, C. T. Ng, J. L. Forand, D. P. Levac, R. E. Mitchell, A. Sen, D. B. Miko, and J. W. McGowan, Phys. Rev. Lett. 50, 335 (1983).

⁷D. S. Belić, G. H. Dunn, T. J. Morgan, D. W. Mueller, and C. Timmer, Phys. Rev. Lett. 50, 339 (1983).

⁸Model 202-Ag-1, Hughes Aircraft Co., Electron Dynamic Division, Torrance, Cal.

⁹P. T. Kirstein, G. S. Kino, and W. E. Waters, *Space Charge Flow* (McGraw-Hill, New York, 1965), p. 153.

¹⁰H. A. Bethe and E. E. Salpeter, *Quantum Mechanics of One and Two Electron Atoms* (Springer-Verlag, Berlin, 1957), p. 238.

¹¹D. McLaughlin and Y. Hahn, private communication.

¹²*Atomic Energy Levels and Grotrian Diagrams*, edited by S. Bashkin and J. O. Stoner, Jr. (North-Holland, Amsterdam, 1975), Vol. 1.